4^{th} *URSI AT-RASC, Gran Canaria, 19 – 24 May 2024*

Interference and Noise Effects on Spectral Moments of Mode-Stirred Reverberation Fields

Luk R. Arnaut*(1), John M. Ladbury(2)
(1) Queen Mary University London, UK
(2) National Institute of Science and Technology, Boulder, CO, USA

Abstract

The effect of harmonic interference (EMI) and bandlimited white noise on the spectral density function of a mode-stirred reverberation field is characterized. Expressions showing the effect on the bandwidth and kurtosis of the stir spectrum are derived and illustrated with numerical results.

1 Introduction

In recent work [1, 2], it was shown how field spectral density functions (SDFs) of a complex electric field $E(\tau)$ can be modelled analytically, for the continuous stir sweep and for its sampled version typically obtained using a vector network analyzer (VNA) or vector spectrum (VSA) analyzer. The corresponding power SDF for a trace obtained using a power sensor can also be deduced.

Similar to probability density functions (PDFs) constituting their probabilistic counterpart in the stir (τ-) domain, SDFs in the spectral stir (ϖ-) domain provide a full characterization of the stir process in terms of the distribution of the amplitude and its RMS fluctuation across ϖ. Since high stir frequency content corresponds to high rates of fluctuation in the stir sweep, the tail of the SDF (and, particularly, the rate of decay in this tail) is a signature of stir efficiency in the randomization process. The spectral kurtosis [1] is a statistic representative of such spectral tail content. With regard to stir efficiency, the the SDF tail varies in an opposite manner to tail of the PDF, as less inefficient (imperfect) stir process exhibits a shorter SDF tail but a heavier PDF tail.

On the other hand, the autocorrelation function (ACF) and autospectral density function (ASDF) form a Fourier transform pair. This implies that the behavior of the ACF at exceedingly short lags (i.e., well below the correlation length; $|\tau| \ll \tau_0$) relates to the ASDF ϖ-dependence at exceedingly high stir frequencies. As a result, in a well-stirred process, short lags in the ACF give rise to rapid drops of correlation levels and strong curvature near zero lag, but this may be easier to identify and characterize across large stir bandwidths at high stir frequencies. This makes the ASDF an attractive alternative to the ACF.

In practice, in evaluation of chamber performance or in EMC testing, one often limits the characterization to a statistic of the PDF or SDF, rather than the completely density function itself, particularly when the number of independent samples is relatively low [3]. For example, in validating the operation of reverberation chambers, a field nonuniformity metric based on the standard deviation or field anisotropy is used in lieu of the PDF when the number of stir states N_s in the τ-domain is relatively low [3]. Similarly for SDFs, the spectral characterization can be limited to a few of its low-order spectral moments [1] when the spectral unit step $\Delta\varpi = 2\pi/N_s$ is relatively large that results in a coarse SDF.

In the evaluation of spectral statistics, one question that arises in validation and EMC testing, then, is the effect of (stir) noise and/or interference on the main spectral moments. The effect of noise was analyzed in [1]. Here, we focus on the effect of EMI, with or without additional noise, represented by a deterministic periodic signal originating from an EUT or the ambient. For simplicity, a single harmonic spectral line is considered; extension to multiple harmonics follows as a straightforward extension.

Fig. 1 shows an example of an experimental SDF at a relatively low CW excitation frequency ($f = 2$ GHz), suffering from the presence of weak EMI and noise at relatively high stir frequencies ($\varpi_k/\Delta\varpi > 1200$).

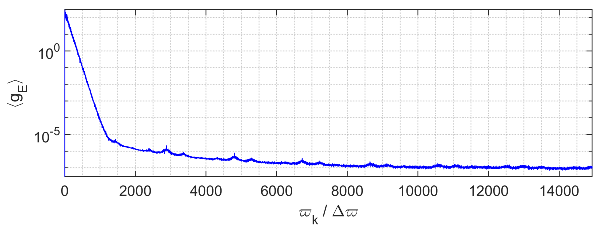

Figure 1. Ensemble averaged ASDF $\langle g_E(\varpi_k/\Delta\varpi)\rangle$ measured at $f = 2$ GHz inside a mode-stirred reverberation chamber. Ensemble realized by 72 secondary tune states.

2 Stir Spectral Moments

For a stir sweep of a continuous complex electric random field $E(\tau) = E'(\tau) + jE''(\tau)$ with zero mean, variance σ_E^2 and normalized one-sided analytic SDF $g_E(\varpi \geq 0) = G_E(\varpi \geq 0)/\sigma_E^2$, the mth-order spectral moments λ_m are related to the autocovariance of its nth- and pth-order time derivatives, viz.,

$$\lambda_m \triangleq \sigma_E^2 \int_0^{+\infty} \varpi^m g_E(\varpi) \mathrm{d}\varpi = \sigma_E^2 \int_{-\infty}^{+\infty} |\varpi|^m s_E(\varpi) \mathrm{d}\varpi \tag{1}$$

$$= \mathrm{j}^{-n}(-\mathrm{j})^{-p} \overline{E^{(n)}(\tau) E^{*(p)}(\tau)}, \quad n+p=m=0,1,2,\ldots \tag{2}$$

Here, the overline in (2) denotes sample path averaging, i.e., taken across a single stir sweep of the primary mode stirrer. For arbitrary m, the λ_m are sample values taken from an ensemble of random Λ_m as generated, e.g., by a secondary stirrer or tuner, with a PDF $f_{\Lambda_m}(\lambda_m)$. Correspondingly, $g_E(\varpi)$ is a sample SDF from an ensemble $G_E(\varpi)$ generated by a secondary mode stirring or tuning. For reasons clarified in [1], we choose $n = p = m/2$ in (2).

At a sufficiently high CW excitation frequency f, for a near-ideal random centered stirred $E(\tau)$ characterized by a quasi-circular Gaussian PDF in the absence of an unstirred line-of-sight contribution and with negligible noise, its SDF has been found [1] to closely attain the form

$$g_{E_s}(\varpi) = \exp(-\varpi/\mathscr{B}_s)/\mathscr{B}_s, \quad \varpi > 0 \tag{3}$$

where $\mathscr{B}_s$ is the stir spectral bandwidth in units rad/s.

In this paper, we focus on the autospectral density function (ASDF) of the form (3) and its spectral moments of even order, which in this case are given by

$$\lambda_m/\lambda_0 = m!\,\mathscr{B}_s^m, \quad m = 0,2,4\ldots \tag{4}$$

and negligible odd-order moments. Extended results for the sample cross-spectral density can be found in [1].

3 Influence of Harmonic EMI

Let $G_E(\varpi) = \sigma_E^2 g_E(\varpi)$ represent the non-normalized single-sided SDF of E. On application of Bochner's theorem for the linear superposition of a noise-free ideal stirred field $E_s(\tau)$ and an interference harmonic field $E_h(\tau)$ of spectral amplitude $\mathscr{E}_{h,0}$, i.e.,

$$E(\tau) = E_s(\tau) + E_h(\tau) \tag{5}$$

$$G_E(\varpi) = G_{E_s}(\varpi) + G_{E_h}(\varpi) \tag{6}$$

In the spectral domain, the harmonic EMI field $\mathscr{E}_h(\varpi) = \mathscr{E}_{h,0}\delta\exp(\mathrm{j}varpi_h))$ provides a discrete contribution

$$g_{E_h}(\varpi) = \delta(\varpi - \varpi_h) \tag{7}$$

to the SDF of $E(\tau)$. The SDF of $E(\tau)$ is

$$\sigma_E^2 g_E(\varpi) = \sigma_{E_s}^2 g_{E_s}(\varpi) + |\mathscr{E}_{h,0}|^2 g_{E_h}(\varpi) \tag{8}$$

whence its mth-order moments follow as

$$\frac{\lambda_{m,E}}{\lambda_{0,E}} = m!\,\mathscr{B}_s^m \frac{\sigma_{E_s}^2}{\sigma_E^2} + \varpi_h^m \frac{|\mathscr{E}_{h,0}|^2}{\sigma_E^2} \tag{9}$$

$$= m!\,\mathscr{B}_s^m \frac{1+\gamma_{E_h}^2 \gamma_{\varpi_h}^m/m!}{1+\gamma_{E_h}^2} \tag{10}$$

in which

$$\gamma_{\varpi_h} \triangleq \varpi_h/\mathscr{B}_s, \quad \gamma_{E_h} \triangleq |\mathscr{E}_{h,0}|/\sigma_{E_s} \tag{11}$$

represent interference-to-stir ratios (ISRs) for frequencies (widths) and amplitudes (RMS levels), respectively. The ASDF bandwidth $\mathscr{B}_E$ and excess kurtosis κ_E' of $g_E(\varpi)$ with reference to the double-sided version of (3) are then

$$\mathscr{B}_E = \sqrt{\frac{\lambda_{2,E}}{2\lambda_{0,E}}} = \mathscr{B}_s \sqrt{\frac{1+\gamma_{E_h}^2\gamma_{\varpi_h}^2/2}{1+\gamma_{E_h}^2}} \tag{12}$$

$$\kappa_E' = \frac{\lambda_{4,E}\lambda_{0,E}}{6\lambda_{2,E}^2} - 1 = \frac{\gamma_{E_h}^2}{\left(1+\gamma_{E_h}^2\gamma_{\varpi_h}^2/2\right)^2}\left(1-\gamma_{\varpi_h}^2+\frac{\gamma_{\varpi_h}^4}{24}-\frac{5\gamma_{E_h}^2\gamma_{\varpi_h}^4}{24}\right) \tag{13}$$

Figs. 2 and 3 show maps for values of $\mathscr{B}_E/\mathscr{B}_s$ and $|\kappa_E'|$ as functions of γ_{E_h} and γ_{ϖ_h}. Loci of points where ideal values $\mathscr{B}_E/\mathscr{B}_s = 1$ or $\kappa_E' = 0$ for $(\gamma_{E_h},\gamma_{\varpi_h}) \neq (0,0)$ are observed.

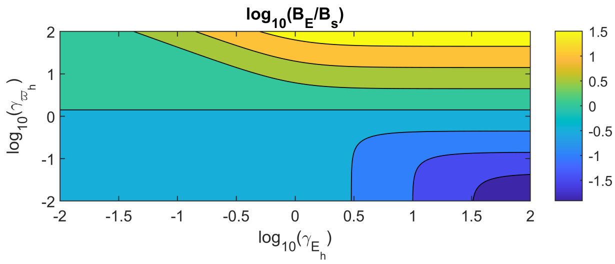

Figure 2. Normaiized bandwidth $\log_{10}(\mathscr{B}_E/\mathscr{B}_s)$.

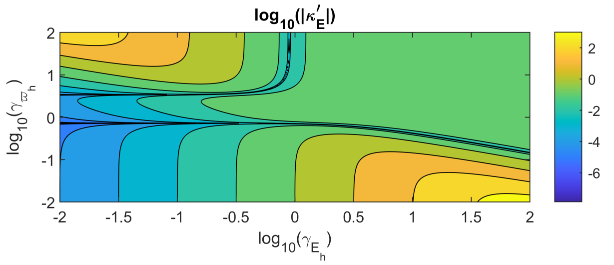

Figure 3. Spectral kurtosis $\log_{10}(|\kappa_E'|)$.

4 Influence of Harmonic EMI and Noise

The previous results can be extended to the case where additive bandlimited white noise is also present. Consider a single harmonic additional field of frequency ϖ_h and independent noise with $g_N(\varpi) = 1/\mathscr{B}_N$ for $0 < \varpi \leq \mathscr{B}_N$ and zero otherwise, leading to

$$E(\tau) = E_s(\tau) + E_h(\tau + N(\tau)) \tag{14}$$

$$\sigma_E^2 g_E(\varpi) = \sigma_{E_s}^2 g_{E_s}(\varpi) + |\mathscr{E}_{h,0}|^2 g_{E_h}(\varpi) + \sigma_N^2 g_N(\varpi). \tag{15}$$

The mth-order moment of E follows as

$$\frac{\lambda_{m,E}}{\lambda_{0,E}} = m!\,\mathscr{B}_s^m \frac{\sigma_{E_s}^2}{\sigma_E^2} + \varpi_h^m \frac{|\mathscr{E}_{h,0}|^2}{\sigma_E^2} + \frac{\mathscr{B}_N^m}{m+1}\frac{\sigma_N^2}{\sigma_E^2} \tag{16}$$

$$= m!\,\mathscr{B}_s^m \frac{1+\gamma_{E_h}^2\gamma_{\varpi_h}^m/m! + \gamma_N^2\gamma_{\mathscr{B}_N}^m/(m+1)!}{1+\gamma_{E_h}^2+\gamma_N^2} \tag{17}$$

in which

$$\gamma_{\mathscr{B}_N} \stackrel{\Delta}{=} \mathscr{B}_N/\mathscr{B}_s, \quad \gamma_N \stackrel{\Delta}{=} \sigma_N/\sigma_{E_s} \tag{18}$$

represent noise-to-stir ratios (NSRs) for bandwidths and amplitudes (RMS levels), respectively. The ASDF bandwidth is now

$$\mathscr{B}_E = \mathscr{B}_s \sqrt{\frac{1+\gamma_{E_h}^2\gamma_{\varpi_h}^2/2+\gamma_N^2\gamma_{\mathscr{B}_N}^2/6}{1+\gamma_{E_h}^2+\gamma_N^2}}. \tag{19}$$

For the excess kurtosis, apart from superimposing terms that are proportional to $\gamma_{E_h}^2$ and γ_N^2, respectively, κ_E' now also contains a nonlinear contribution by cross-coupling between the EMI and noise, i.e.,

$$\begin{aligned}\kappa_E' = &\left(1+\frac{\gamma_{E_h}^2\gamma_{\varpi_h}^2}{2}+\frac{\gamma_N^2\gamma_{\mathscr{B}_N}^2}{6}\right)^{-2}\\ &\times\left[\gamma_{E_h}^2\left(1-\gamma_{\varpi_h}^2+\frac{\gamma_{\varpi_h}^4}{24}-\frac{5\gamma_{E_h}^2\gamma_{\varpi_h}^4}{24}\right)\right.\\ &+\gamma_N^2\left(1-\frac{\gamma_{\mathscr{B}_N}^2}{3}+\frac{\gamma_{\mathscr{B}_N}^4}{120}-\frac{7\gamma_N^2\gamma_{\mathscr{B}_N}^4}{360}\right)\\ &\left.+\gamma_{E_h}^2\gamma_N^2\left(\frac{\gamma_{\varpi_h}^4}{24}+\frac{\gamma_{\mathscr{B}_N}^4}{120}-\frac{\gamma_{\varpi_h}^2\gamma_{\mathscr{B}_N}^2}{6}\right)\right].\end{aligned} \tag{20}$$

5 Conclusion

Spectral bandwidth and kurtosis offer simple but powerful spectral statistics with which the effect of EMI and/or noise on the SDF of a stir process can be evaluated for diagnostics. However, care must be exercised in interpreting their value. As numerical results in Figs. 2 and 3 indicate, spurious ideal values of $\mathscr{B}_E = \mathscr{B}_s$ and/or $\kappa_E' = 0$ arise at certain pairs $(\gamma_{E_h}, \gamma_{\varpi_h})$. These are a result of competition between the ISR of frequencies vs. levels (RMS amplitudes), which have opposing effects of raising and lowering the spectral bandwidth and kurtosis. This situation parallels the one encountered for pure noise effects arnacorrpsdf. The combined presence of EMI and noise compounds the issue.

References

[1] L. R. Arnaut and J. M. Ladbury, "Correlation and spectral density functions in mode-stirred reverberation," *IEEE Trans. Electroagn. Compat.*, submitted for publication, 2023.

[2] L. R. Arnaut and J. M Ladbury, "Correlation and spectral density functions for dynamic stochastic fields," *Proc. URSI GASS 2023*, Sapporo, Japan, 19 – 26 Aug. 2023.

[3] Electromagnetic Compatibility (EMC): Part 4: Testing and Measurement Techniques: Section 21: Reverberation Chambers, International Electrotechnical Commission Standard JWG REV SC77B-CISPR/A, IEC 61000-4-21. Geneva, Switzerland, 2nd ed., Jan. 2011.